# HYDROMAGNETIC INSULATION IN BLACKJACK III DIODE

Andrew Wilson and Mark C. Friedman
Systems, Science and Software
P.O. Box 1620, La Jolla, CA 92038

## Introduction

In Z-pinch experiments a strongly radiating plasma may adversely effect the transport of power delivered to it. Plasma generated x-rays cause ablation of the diode walls and, if the walls do not become good conductors or if the current (I) carried in the electrode surfaces is too small, loss of insulation in the diode can result. Last year we interpreted experimental results at Maxwell Laboratories[1] as evidence for hydrodynamic closure and proposed a theory to explain the reported behavior. While the explanation was qualitatively correct there were no measurements that could be compared to a detailed quantitative analysis. The work described here presents the theoretical model used to design, and be compared with, recent experiments on BLACKJACK III (BJ3) at Maxwell Laboratories.

These experiments are required to validate the theory so that the effects of closure can be predicted for present and future SHIVA configurations, diodes, and plasma loads.

## Analysis of BLACKJACK III Experiments

### Experimental Geometry

Figure 1 shows a cylindrical plasma irradiating the surfaces which carry current to and from it. This double-disk geometry is the simplest one in which to analyze the radiatively driven ablation and during the design phase for these experiments it was selected as providing a reasonable high power inductive diode while simultaneously providing a configuration in which (a) the radiative transport was not too complicated and (b) the blow-off from the electrodes could be seen and measured easily.

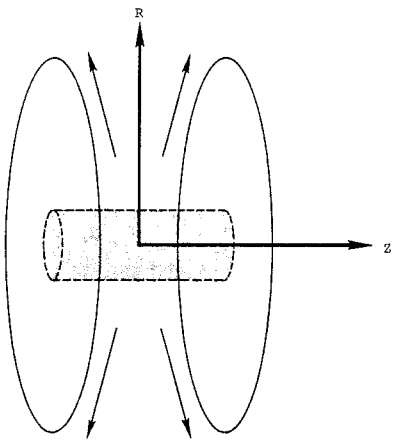


Figure 1. Double-disk geometry schematic.

The experimental configuration is shown in Figure 2. The load for the diode is an array of thin wires which, on imploding, emit an intense burst of x-rays. The diode itself consists of two parallel, flat disks (aluminum or copper) approximately 25 cm in diameter. With this configuration it is possible to have unobstructed view of the plasma as well as the movement of the electrode surfaces.

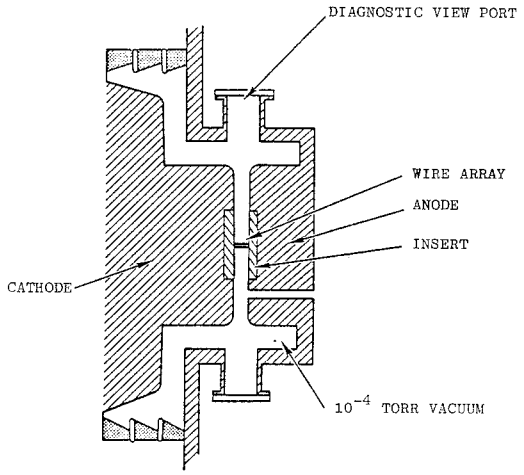


Figure 2. BLACKJACK III vacuum diode.

Visual diagnostics include streak photography as well as laser shadowgraphy. The streak photograph information turns out to be very difficult to interpret and, in general not useful for this experiment. The laser shadowgraph information, on the other hand, gives information about the lowest density parts of the ablating plasma which is useful for comparison purposes.

### Computational Model

The model used to describe the interaction of the x-rays with the walls has to include the following features: (a) x-ray transport in the vacuum region; (b) energy diffusion into the walls; (c) opacity and equation of state information for the wall material; (d) hydrodynamics of the walls; (e) magnetic forces on the expanding walls. To do this we used a version of the MRVERA code[2] which was modified to include the magnetic field terms ($\vec{J}x\vec{B}$ force, joule heating, Ohm's Law, Faraday's Law, Ampere's Law) and thermal conduction. The individual sections of the wall were treated locally as one-dimensional but they were coupled through the two-dimensional features of the vacuum radiation transport. Extensive use was made of the CAPO[3] generated equation of state and opacity data for the electrode materials (aluminum, plastic and copper).

### Preliminary Calculations

The x-ray output and diode wall current histories are shown in Figure 3. In the initial calculations the area under the power curve was 8 kJ (this turned out to be too large) and $I_{max}$ was 0.6 MA. The gap separating the disks was 2 cm.

Figure 4 shows the diode geometry as well as the calculational regions' surface

# Report Documentation Page

*Form Approved*
*OMB No. 0704-0188*



| 1. REPORT DATE | 2. REPORT TYPE | 3. DATES COVERED |
|---|---|---|
| **JUN 1981** | **N/A** | **-** |

| 4. TITLE AND SUBTITLE | 5a. CONTRACT NUMBER |
|---|---|
| **Hydromagnetic Insulation: In Blackjack III Diode** | 5b. GRANT NUMBER |
| | 5c. PROGRAM ELEMENT NUMBER |
| 6. AUTHOR(S) | 5d. PROJECT NUMBER |
| | 5e. TASK NUMBER |
| | 5f. WORK UNIT NUMBER |
| 7. PERFORMING ORGANIZATION NAME(S) AND ADDRESS(ES) **Systems, Science and Software P.O. Box 1620, Ln Jolla, CA 92038** | 8. PERFORMING ORGANIZATION REPORT NUMBER |
| 9. SPONSORING/MONITORING AGENCY NAME(S) AND ADDRESS(ES) | 10. SPONSOR/MONITOR'S ACRONYM(S) |
| | 11. SPONSOR/MONITOR'S REPORT NUMBER(S) |

12. DISTRIBUTION/AVAILABILITY STATEMENT
**Approved for public release, distribution unlimited**

13. SUPPLEMENTARY NOTES
**See also ADM002371. 2013 IEEE Pulsed Power Conference, Digest of Technical Papers 1976-2013, and Abstracts of the 2013 IEEE International Conference on Plasma Science. Held in San Francisco, CA on 16-21 June 2013. U.S. Government or Federal Purpose Rights License.**

14. ABSTRACT

15. SUBJECT TERMS

| 16. SECURITY CLASSIFICATION OF: | | | 17. LIMITATION OF ABSTRACT | 18. NUMBER OF PAGES | 19a. NAME OF RESPONSIBLE PERSON |
|---|---|---|---|---|---|
| a. REPORT **unclassified** | b. ABSTRACT **unclassified** | c. THIS PAGE **unclassified** | **SAR** | **4** | |

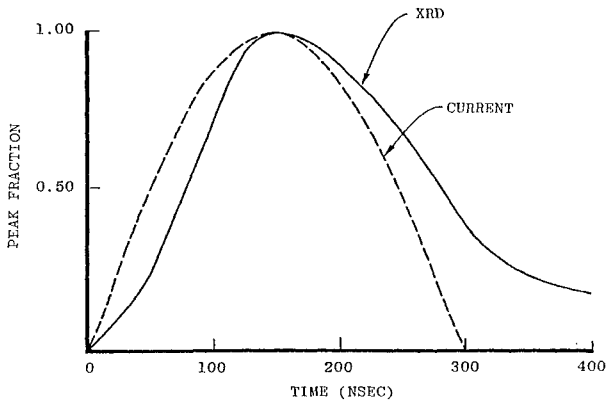


Figure 3. Normalized XRD and current pulseforms.

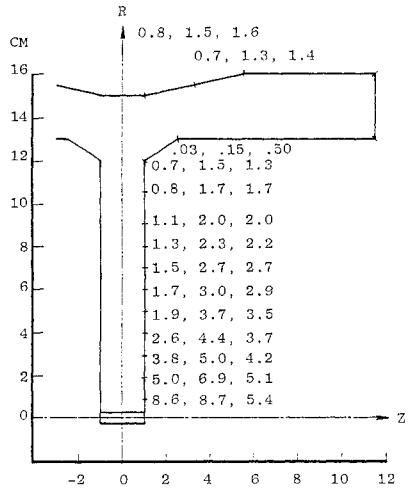


Figure 4. Plasma surface temperature (in eV) at 115, 200, and 370 ns, respectively.

temperature ($\theta$) at three times. The relatively cool temperatures ($\sim$5 eV) result in the emission of very soft x-rays in the 10 to 20 eV band with an appreciable fraction radiated in the visible.

An interesting feature which resulted from these calculations is the ablation front's non-monotonic dropoff with radius (r), shown in Figure 5. Early in the pulse, before the magnetic field (B) builds up and its $1/r^2$ dependence dominates, blow-off is most rapid close to the source. Later the B field increase is enhanced by the hotter plasma there being a good conductor, thus preventing magnetic diffusion from taking place and producing steep gradients in the magnetic force, $\partial/\partial z\ (B^2/8\pi)$. At late times B has dropped off and ceases to restrain the plasma. Farther from the source the weaker B, coupled with a cooler more resistive plasma, has less and less effect on the hydrodynamic motion. For this geometry the flux, (energy/cm$^2$/sec) normal to the surface drops off as $\sim(1/r)^3$ for large r. Thus at larger r the material $\theta$ and blowoff velocity ($v_f$) are reduced.

A simple quasi-analytic model described in a recent report[4] can be used to further

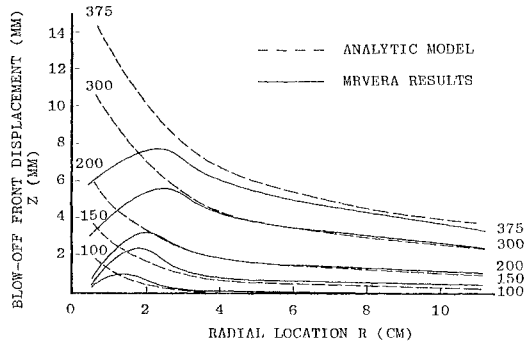


Figure 5. Blow-off front along 2 cm gap BJ3 disk diode.

understand the phenomenology. If the magnetic field pressure can be neglected (i.e., far from the source), the velocity ($v_f$) of the ablation front exposed to an incident radiant flux, dE/dt, can be parameterized as $v_f = v_f(E)$, where E is the energy (J/cm$^2$) that has entered the material after front surface vaporization has occurred. Separate radiation hydrodynamic calculations yielded the dependence $v_f \sim 2.58\ E^{2/9}$ cm/$\mu$sec, which holds (in A$\ell$) over a wide range of conditions.

To compute $v_f$ in a simple manner the regions are assumed to receive energy directly from, and only from, the source. Neglect of re-emission may be quite a good approximation for regions that are cold compared to the source. Figure 5 shows the analytic blow-off front profile histories compared to those calculated with a magnetic field and re-emission by MRVERA. Beyond r = 3 cm the analytic treatment performs well showing good agreement during the MRVERA calculational time span for the far field regions where the influence of B was expected to be slight.

## Interpretation of Visible Streak Data

The visible streak photographs give clear evidence for the expansion of both cathode and anode surfaces and for the closing of the diode gap. Figure 6 shows the displacement of the ablation front with respect to the original cathode and anode surfaces observed from a visible streak on BJ3. The difference in the cathode and anode blow-off rates are slight, probably due to misalignment and not considered to be experimentally significant. It is clear that the expansion rate is fairly constant between 100 and 200 nanoseconds (ns). Thereafter it slows down or comes to a halt. This behavior is not expected theoretically (Figure 5).

The reason for this behavior, it turns out, is based on the interpretation of what is observed. Briefly, the visible streak photographs do not provide direct information about the displacement of the electrode surfaces. Rather, as we have shown elsewhere,[5] they provide information about the more strongly emitting regions of the plasma. Beyond this, considerable unfolding is required to obtain anything that is useful for comparison purposes.

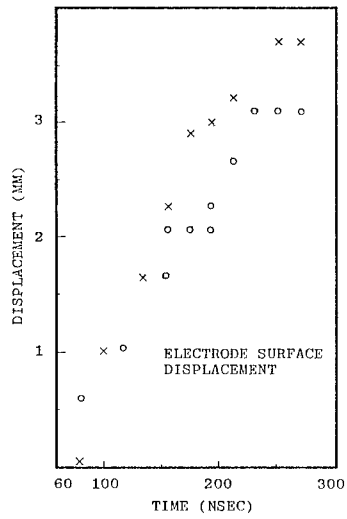


Figure 6. Displacements observed in BJ3 along the chord y = 1.5 cm (visible streak photographs).

Interpretation of Laser Shadowgraph Results

The other experimental diagnostic which was used in the BLACKJACK III experiments was a laser shadowgraph. In this technique a visible laser provides the source to be measured; whereas, the visible streak relied on material emission sources. The advantage of this scheme is that the top of the ablated layer can now be seen. Even at densities where the material is no longer opaque it can be "seen" because the medium refracts the visible light passing through it. The light that is strongly refracted due to large electron density ($n_e$) gradients will not show up on the receiving system. The technique highlights strong $n_e$ gradients and is thus reliable for observing the ablation front if it is not too diffuse.

The shadowgraph method was used with the double-disk geometry with radial viewing, as shown in Figure 2, and shadowgraphs were snapshot at intervals of 30-50 ns. It was used with Aℓ, brass, and Cu electrodes and almost entirely with diode gaps of 1 cm at atmospheric pressure and 8 mm under vacuum conditions.

MRVERA performed calculations using Cu electrodes and an 8 mm gap. The energy under the power curve (Figure 3) was the measured value of 2.5 kJ. Figure 7 shows a comparison of measurements on Cu, brass, and Aℓ with the calculated results for Cu. The maximum displacement ($\Delta z$) of the anode and cathode surfaces are plotted as a function of time. These points are special in the sense that they are unobscured by material in the line of sight. The radial positions corresponding to the points indicated are, in general, time-dependent. This is to be expected since, in Figure 5, $\Delta z_{max}$ occurs at larger r late in the pulse. Agreement between theory and experiment is remarkably good, considering the complexities of the underlying physics.

Not shown here are the projected radial profiles of the shadowgraph. We did not

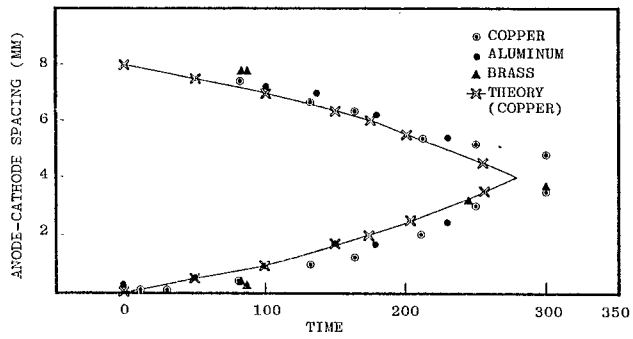


Figure 7. Comparison of theory and experiment for the maximum ablation front displacement of electrode surfaces in BJ3 (laser shadowgraph).

analyze these since it is a major task to unfold the measurements and relate them to calculated quantities. However, those profiles do exhibit the non-monotonic dropoff of displacement amplitude z(r) with radius.

It is interesting that the cathode and anode blow-off are not quite symmetric. Our theory says that if the plasma source is uniform across the gap then both should show equal expansion. A possible explanation for the slight asymmetry is the difficulty which is intrinsic to aligning the laser apparatus and the beam parallel to the electrode surface. Deviations from perfect alignment could result in the observed results. The angle subtended by the blow-off is $\Delta\theta \sim 2$ mm/100 cm $\sim 2 \times 10^{-3}$ radians or a tenth of a degree. The asymmetry errors involve even smaller angles.

The other feature which shows deviation from theory occurs late in the pulse. Theory predicts closure; whereas, the experimental results show a slowing of the closure rate. We suspect the reason for this is again the difficulties of the experiment. Until 150 or 200 ns the B field ensures that the $n_e$ is very steep near the blow-off front (Figure 8) so that the shadowgraph technique is ideal.

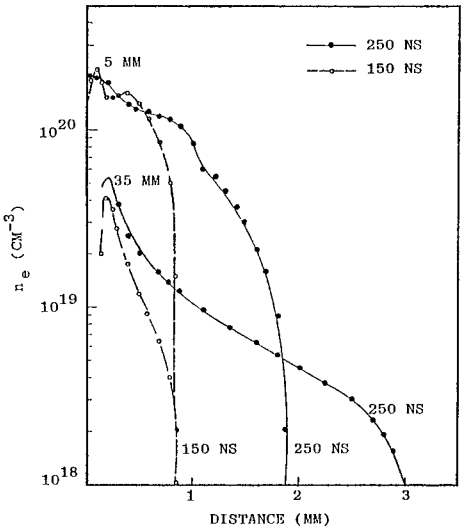


Figure 8. Electron density profiles at the radial positions indicated both early and late in the pulse.

Later, I and B drop and the front expands and becomes quite diffuse. The reduced $n_e$ gradients are much more difficult to measure and, we suspect, the refraction too weak to indicate the low $n_e$ front location.

Agreement between calculations and measurements for Cu is excellent. However, measurements for Aℓ and brass electrodes are not markedly different. Reasons for this behavior are discussed elsewhere.[6,7] Reference 6 also examines the effects of surface contaminants.

## Conclusions

We have demonstrated that for high power diodes in which the load is not passive but emits x-rays, the wall electrodes undergo extensive ablation. The effect is thus important in all high power Z-pinch experiments in plasmas. We have seen how closure could take place and, while in these experiments complete closure did not occur until late in the pulse due to a careful choosing of the pulse length and gap width, it is clear that without special precautions closure can occur during experiments.

Even without the complete closure of the diode the power transfer to the load can be affected appreciably. That is, the local inductance (per unit length) or, equivalently, the local line impedance, is altered by the moving electrode surfaces. This, in turn, modifies the voltage and hence the current carried. The effect is discussed elsewhere.[8]

The computational model appears to have been verified by experiment. This is an impressive achievement in a physical regime where the transport coefficients, opacities, etc. are somewhat suspect. Moreover, the results obtained show that the radiation-MHD techniques used to compute fluid behavior in this very high aspect ratio geometry are valid. This provides encouragement for theoretically predicting the closure properties of x-ray diodes and for designing them for specified radiating loads. It also provides incentive for checking the thermodynamic, electrical, and opacity behavior of materials other than those considered here. Finally, the results show that the laser shadowgraph (or holograph) technique is invaluable for observing these cool diffuse plasmas and is superior to visible streak diagnostic photographs.

## Acknowledgment

This work was supported by the Air Force Weapons Laboratory as a subcontract to Maxwell Laboratories.

The authors wish to thank J. Pearlman, J. Shannon and A. Perratt of Maxwell Laboratories and R. Reinovsky of AFWL for their cooperation during the course of this work and for permitting us to show their experimental data.

## References

1. Wilson, A., et al., Systems, Science and Software Report SSS-R-80-4148, August 1979.

2. Bailey, L. E., S. Peyton and M. C. Friedman, Defense Nuclear Agency Report DNA 2951T, March 1972.

3. Katz, I., R. Vik and J. Harvey, Defense Nuclear Agency Report DNA 3600F-1, June 1975.

4. Wilson, A., et al., Systems, Science and Software Report SSS-R-80-4517, June 1980.

5. Brannon, J., et al., A. Wilson and M. C. Friedman, Maxwell Laboratories Report MLR-1050, January 1981.

6. Wilson, A. and M. C. Friedman, Systems, Science and Software Report SSS-R-81-4780 December 1980.

7. Wilson, A. and M. C. Friedman (4th International Conference on High Power Electron and Ion-Beam Research and Technology Palaiseau, France, July 1981).

8. Waisman, E. M. and M. Chapman, Systems, Science and Software Report SSS-R-81-4960 April 1981.